Separation Science and Technology
Publication details, including instructions for authors and subscription information:
http://www.informaworld.com/smpp/title~content=t713708471

Production of Polyethersulfone Hollow Fiber Ultrafiltration Membranes. I. Effects of Water (internal coagulant) Flow Rate (WFR) and Length of Air Gap (LAG)

Xiangqun Miao[a]; S. Sourirajan[a]; H. Zhang[a]; Wayne W. Y. Lau[a]
[a] DEPARTMENT OF CHEMICAL ENGINEERING, NATIONAL UNIVERSITY OF SINGAPORE, SINGAPORE

To cite this Article Miao, Xiangqun , Sourirajan, S. , Zhang, H. and Lau, Wayne W. Y.(1996) 'Production of Polyethersulfone Hollow Fiber Ultrafiltration Membranes. I. Effects of Water (internal coagulant) Flow Rate (WFR) and Length of Air Gap (LAG)', Separation Science and Technology, 31: 2, 141 — 172
To link to this Article: DOI: 10.1080/01496399608000687
URL: http://dx.doi.org/10.1080/01496399608000687

SEPARATION SCIENCE AND TECHNOLOGY, 31(2), pp. 141–172, 1996

Production of Polyethersulfone Hollow Fiber Ultrafiltration Membranes. I. Effects of Water (internal coagulant) Flow Rate (WFR) and Length of Air Gap (LAG)

XIANGQUN MIAO,* S. SOURIRAJAN, H. ZHANG, and WAYNE W. Y. LAU
DEPARTMENT OF CHEMICAL ENGINEERING
NATIONAL UNIVERSITY OF SINGAPORE
10 KENT RIDGE CRESCENT, SINGAPORE 0511

ABSTRACT

The effects of water flow rate (WFR) (5 or 7.5 mL/min) and length of air gap (LAG) (in the range of 50 to 120 cm) on the characteristics of hollow fiber membranes produced by the solution spinning technique using two polymer solution compositions C1 and C2, were studied experimentally. The polymer (polyethersulfone), solvent (1-methyl-2-pyrrolidone), and additive (polyvinyl pyrrolidone) concentrations (wt%) were 20, 75, and 5 respectively for the C1 solution, and 20, 70, and 10 respectively for the C2 solution. The viscosity of the C1 solution used was 2112 cP and that of the C2 solution used was 3924 cP. The extrusion pressures (EP) were 5 and 15 psig, respectively, for fiber production from the C1 and C2 solutions. The effect of higher solution viscosity, together with higher EP, was to increase both the outside diameter (OD) and the inside diameter (ID) for C2 fibers. For both C1 and C2 fibers, an increase in WFR at a given LAG tended to increase OD and ID and to decrease wall thickness, whereas an increase in LAG at a given constant WFR tended to decrease OD, ID, and wall thickness for the resulting fibers. The UF separation (%) of PEG solutes (of different molecular weights) in dilute aqueous solutions and the membrane permeated product rates (PR, g/cm^2·h) at the average operating pressure of 20 psig were also examined as functions of WFR and LAG. Data on C1 fibers showed that for the case of WFR = 5 mL/min, an increase in LAG tended to increase both PEG separations and

* To whom correspondence should be addressed. The author's previous name was Miao Siang Qun.

PR; at WFR = 7.5 mL/min, an increase in LAG tended to increase PEG separations but to decrease PR. The data on C2 fibers showed that both PEG separations and PR increased with an increase in LAG, and decreased with an increase in WFR. All the above results are discussed from the points of view of the physicochemical events of desolvation, fiber swelling, and fiber stretching taking place during fiber production.

INTRODUCTION

Hollow fiber (HF) membrane offers two major advantages over flat or tubular membranes: 1) they have higher membrane area, and hence higher productivity, per unit volume of membrane module; and 2) they are self-supporting. For these two reasons the HF membrane configuration is currently the preferred choice for membrane separation applications wherever possible. Polymer HF membranes, with or without surface modification, are especially versatile in utility for a wide variety of low pressure applications such as ultrafiltration (UF), microfiltration, pervaporation, gas–vapor, and gas–gas separations. For the above reasons, technology development research in the production of HF membranes is of practical industrial interest. This work is part of such research with respect to polyethersulfone (PES) UF membranes.

Published literature reports (1–14) on detailed experimental studies on the cause–effect relationship in membrane-making conditions and data on physical dimensions and UF performance of the resulting membranes are far less extensive with respect to HF membranes compared to, for example, flat sheet cellulose acetate membranes (15). The following is a brief literature review of some relevant aspects of HF membrane research.

The early work of Cabasso et al. (1–6) is by far the most informative. Using PS (polysulfone, Udel 1700 or 3500), DMA (dimethyl acetamide), or DMF (*N*,*N*-dimethylformamide), and PVP (polyvinyl pyrrolidone) in the fiber casting solution, they showed (1) that HF membranes with diverse properties could be successfully spun by the dry-wet spinning process, and the outside diameter (OD) of the fiber increased with an increase in the extrusion rate of the fiber casting solution through the spinnerette.

On parameters governing the morphology of the spun hollow fiber, Cabasso et al. showed (2) that control of the extrusion and/or coagulant procedure allowed the formation of either skinned, porous-skinned, or nonskinned fibers. Use of a powerful nonsolvent as the internal coagulant caused rapid precipitation of polymer from the bore toward the outer periphery, which served as a barrier to the further diffusion of the coagulant through the fiber wall. Consequently, the viscosity of the polymer solution on the outer wall of the nascent fiber remained essentially unchanged when it entered the external coagulant water bath. This led not

only to the formation of large intrusion cells but also some contraction of the internal core which could result in the formation of a fiber within a fiber.

Cabasso et al. (3) found that exposure of fibers to elevated temperature (110°C) for a short period drastically reduced surface pore size and narrowed pore size distribution, whereas overall fiber dimensions were reduced only by 1%; 85% of the fiber's permeability was retained. Cabasso et al. also demonstrated (4) that polysulfone HF membranes with surface pore sizes less than 0.2 μm could be used effectively as substrates for a coating of polyethyleneimine or furan resin to produce composite RO membranes similar to the flat sheet NS-100 and NS-200 membranes (16).

In a more recent report (5), Cabasso pointed out that hollow fibers could be produced from almost any spinnable material. A skin could be formed either on the external or bore side surface of the fiber. By a dry-wet spinning process using PS (Udel 3500, 28 wt%), PVP (MW of 15,000, 15 wt%), and DMA (57 wt%), with water as external and internal coagulant and an air gap of 75 cm at 25°C, Cabasso obtained microvoid-free HF membranes with an external porous skin, the formation of which was attributed to the lower mobility of the high molecular weight PVP relative to that of solvent DMA (6).

According to Mckinney (7), in the dry-wet fiber spinning process, the casting solution may have a polymer concentration in the 20 to 45 wt% range, a solvent concentration in the 55 to 80 wt% range, and the solvent can be single or binary; further, the spin temperature can be in the −15 to 70°C range, and surface-active agent can be used as a coagulant enhancer.

Asymmetric hollow fibers with a skin layer on the outside of the fiber were made by Espenan and Aptel (8). Using a polymer solution composed of PS (Udel 3500), Triton X100, and DMF, they studied the main variables of the spinning process. They noted that membrane permeability could be increased by decreasing the polymer concentration and/or by adding a pore-forming agent to the spinning solution. They pointed out that the dry-wet hollow fiber-making process offered the possibility of changing the properties of the membranes by varying the nature of the core fluid. In order to produce a highly permeable outer skinned hollow fiber, a pore-forming agent of relatively low concentration should be added to the polymer solution, and the solvent for the polymer must be used as the core fluid. The solvent in the inside channel of the nascent fiber has the following three functions:

It keeps the inner channel open
It avoids the formation of an inside skin
It diffuses into and through the polymer solution, lowering its polymer content and reducing the rate of its precipitation

The latter two effects are favorable to the formation of a more porous structure.

Using a spinning solution of PES (23 wt%), PVP (MW 10,000, 12 wt%) and DMA (65 wt%), water as external coagulant, and an air gap of 62 cm, Liu et al. (9) investigated the effect of several internal coagulants (20 wt% aqueous solution of acetic acid, *n*-propionic acid, *n*-butyric acid, sulfuric acid, and formamide) on the pore size and pore size distribution on the bore side of the resulting hollow fibers, analyzing the data on the basis of the surface force–pore flow model (15). Their results showed that the data on the pure water permeation rate (PWP) were in the range 1.09 to 1.70 g/cm^2·h, and the pore sizes were in the range 33 to 44 Å (with a standard deviation σ of 7.3 to 9.8 Å) in the first distribution, and 70 to 83 Å (with σ of 4.5 to 7Å) in the second distribution; the number of pores in the second distribution was 0.6 to 1.3% of that in the first distribution.

In a later investigation Liu et al. (10) studied the effect of PVP and polymer (PES or PS) concentration in the spinning solution (with DMA as solvent), and also the operating variables on the physical dimensions and performance of the resulting HF membranes. They used an air gap of 80 cm, an extrusion pressure of 40 psig, and an internal coagulant water flow rate of 14 to 18 mL/min; ice-cold water was the external coagulant in all cases. Membranes were characterized by data on PWP, and UF separation of PEG solutes of different molecular weights in dilute aqueous solutions, at an operating pressure of 20 psig. They found that an increase in PVP in the spinning solution increased PWP and decreased PEG separations. While an increase in polymer concentration in the spinning solution increased PEG separations for both the PES and PS membranes, the corresponding PWP would increase or decrease depending on the fiber making conditions. Changes in PVP and polymer concentration also changed the physical dimensions of the resulting fibers; further, the length of the air gap had a significant effect on the size, number, and distribution of pores on the bore side of the membrane surface.

Wood et al. (11) pointed out the relevance of the critical polymer concentration on the performance of the fibers obtained from a spinning solution. They showed that PWP gradually decreased and PEG separations increased when PES concentration in the spinning solution exceeded its critical concentration. According to their estimate, the critical concentration of PES in DMA solvent is 0.2229 g/cm^3.

Brinkert et al. (12) studied the relation between compaction and mechanical properties of UF hollow fibers, and concluded that the maximum operating pressure at which no compaction occurred was closely related to the viscoelastic behavior of the membrane material.

A new spinning technology for producing hollow fiber membranes has recently been reported (13, 14). The technique makes use of a new type of

spinnerette having three concentric orifices, and it allows spinning without contact with air. Beside the usual polymer solution and the bore liquid, a third liquid (which serves as the first external coagulant) can be pumped through the outer orifice. After a certain contact time with the third liquid, the nascent hollow fiber meets the second coagulant bath. This technique opens new possibilities for greater control of the morphology of the resulting fiber.

While the literature reviewed above is both instructive and informative, still a more extensive and also a more definite database is needed in order to establish a firm experimental basis for the production of unique membrane products for specific separation applications. It is the object of this work to contribute to the generation of such a database with respect to the production of PES (Victrex) hollow fiber (capillary) UF membranes.

The hollow fibers were produced in this work by the dry-wet solution spinning technique with an experimental arrangement similar to that used by Liu et al. (10). In this work, the fiber spinning solution contained PES as the polymer, NMP (1-methyl 2-pyrrolidone) as the solvent, and PVP (MW 10,000) as the additive. The effects of water (internal coagulant) flow rate (WFR, mL/min), and length of air gap (LAG, cm) on the characterization of the resulting fibers were studied. These characteristics included fiber dimensions, i.e., outside diameter (OD, mm), inside diameter (ID, mm), wall thickness (mm), and OD/ID ratio; fiber morphology (SEM photographs); nascent fiber velocity (NFV, cm/s); and fiber performance as expressed by PR (membrane product rate at 20 psig, g/cm^2·h) and UF separations (f, %) for PEG solutes with different molecular weights in dilute aqueous feed solutions. Cold water (~4°C) was used as the external coagulant, and all fiber production and characterization experiments were carried out at the laboratory temperature (~24°C).

EXPERIMENTAL

Materials

PES (Victrex 4800 P) supplied by Imperial Chemical Industries was initially dried for 3 hours at 150°C and then used. NMP supplied by Merck, PVP (MW 10,000) supplied by Sigma Chemical, and PEG of different molecular weights supplied by Aldrich Chemical and Merck were the other chemicals used in fiber production and testing.

Fiber Spinning Solution

Two solution compositions, C1 and C2, were used for fiber spinning as shown in Table 1. The components were mixed in a 1-L glass bottle with a Teflon cap. The bottle was placed on a roller, and the contents were

TABLE 1
Compositions and Viscosities for C1 and C2 Filtered Solutions

	C1	C2
PES, wt%	20	20
NMP, wt%	75	70
PVP, wt%	5	10
Apparent viscosity, cP	2112	3924

roller mixed for 3 hours. After that, the bottle was kept in an air oven at 60°C overnight. Again, the components were roller mixed for 4 hours everyday for 1 week. Except during mixing, the bottle was kept in the air oven at 60°C for 1 week. It was then left at room temperature for 24 hours, and filtered before use in fiber spinning. The viscosity of each fiber spinning solution was determined at the laboratory temperature using a Haake Viscometer MV Sensor System. The viscosity data given in Table 1 are for the filtered solution used for fiber spinning.

Fiber Spinning

Figure 1 shows a schematic diagram of the fiber spinning apparatus used in this study. The 1-L polymer solution tank (1) was equipped with a safety valve, a thermometer, inlet for high pressure nitrogen, and connection to a vacuum pump. Nitrogen gas from the tank could also be partially released by turning the safety valve manually to adjust the pressure in the tank during the spinning process. A vacuum pump (5) was used to eliminate gas bubbles in the polymer solution before spinning. The filter (15) was a 200-mesh filter disk made by stacking two pieces of a polyester fabric filtration medium to stop suspended particles from entering the spinnerette. The filter assembly was thoroughly cleaned, and the polyester fabric was replaced every time after use. Solution filtration was operationally separate from solution spinning—in other words, the filter system was disconnected from the apparatus prior to solution spinning. To remove the gas bubbles in the polymer solution caused by the filtration process, the filtered solution was placed in the solution tank and evacuated by using the vacuum pump (5) for 1 hour.

The spinnerette has a precision orifice containing a centrally positioned inlet tube (tube-in-orifice, Fig. 2) for the delivery of the internal coagulant medium. The internal coagulant was introduced through the inlet tube to create and control the bore structure of the hollow fiber.

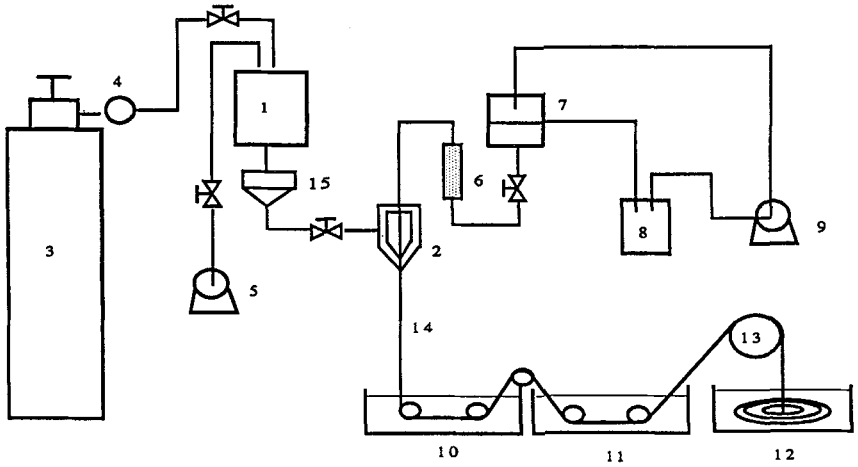

1. Polymer solution tank
2. Spinnerette
3. Nitrogen cylinder
4. Pressure gauge
5. Vacuum pump
6. Rotameter
7. Internal coagulant tank
8. Overflow tank
9. Pump
10, 11 and 12. External coagulant baths
13. Spooling machine
14. Air gap
15. Filter

FIG. 1 Schematic diagram of the apparatus for hollow fiber spinning.

The internal coagulant, which was deionized water at room temperature (~24°C) in this work, passed through a rotameter (6) at a flow rate (WFR) of 5 or 7.5 mL/min (as set), and it flowed through the spinnerette by gravity. To keep a constant hydrostatic head, the internal coagulant tank (7) was open to the atmosphere, and the water was delivered to the tank (7) by a small pump, keeping the water level constant in the tank. The overflow from this tank was collected in the overflow tank (8) which also served as a storage tank for water.

The air space between the spinnerette and the water level in the external coagulant bath (10) is the "air gap." The length of this air gap (LAG) varied from 50 to 120 cm in this study. When LAG was changed, the internal water flow rate was adjusted to keep the WFR reading constant at the preset value.

The polymer solution was extruded through the spinnerette under a nitrogen pressure (EP) of 5 or 15 psig as needed.

After passing through the desired LAG, the extruded nascent hollow fiber entered the external coagulant (water) bath which consisted of three

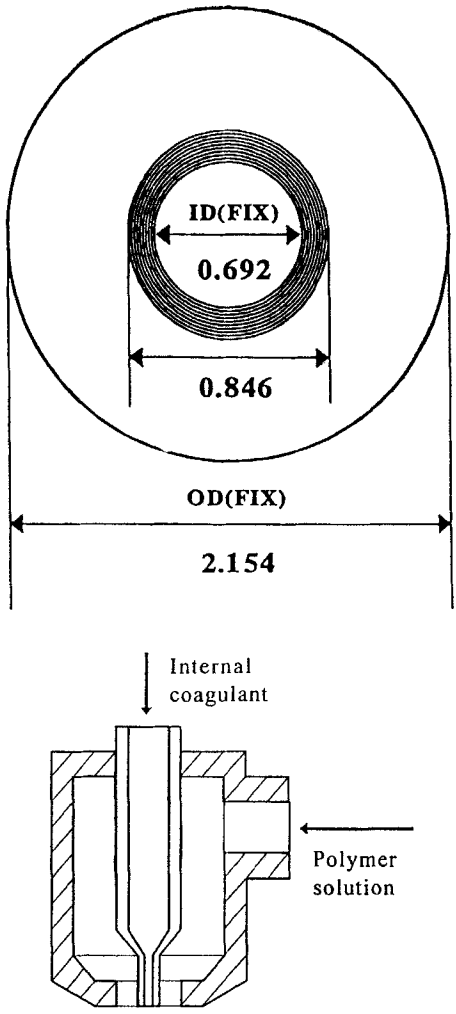

FIG. 2 Top: Schematic diagram of the spinnerette. Bottom: Schematic diagram of cross section of the spinnerette tube-in-orifice. Unit: millimeters.

compartments. The coagulant in the first two compartments (10 and 11) was deionized water at ~4°C, and that in the last compartment (12) was deionized water at room temperature (~24°C). The nascent hollow fiber was guided forward over several rollers (set in the first two compartments) by the spooling machine (13) whose speed could be adjusted in response

to the speed of the nascent fiber formed. Finally, the fiber entered the last water bath where it was collected.

During the fiber spinning process, the nascent fiber velocity (NFV, cm/s) was determined by collecting a sample of well-coagulated fiber length in a known time interval in the final coagulation bath.

Fiber Characterization

The physical dimensions (OD, ID, and wall thickness) of all fibers were measured on microtoned section using an Olympus Vanox microscope, and the cross sectional morphologies of several selected fibers were also examined under a scanning electron microscope (SEM). Further, all fibers were also characterized by their performance in UF experiments in terms of their PWP (pure water permeation rate, $g/cm^2 \cdot h$), PR (membrane permeated product rate, $g/cm^2 \cdot h$) and percent separations of several PEG solutes [MW range 1000 (1K) to 10,000 (10K)] in dilute aqueous feed solutions (PEG concentration, ~100 ppm) at the average operating pressure of 20 psig at the feed flow rate of 1 L/min or higher.

Figure 3 shows a schematic diagram of the HF membrane test system used. In this work the HF bundles were made as follows. Several (four to six) fibers, each 30 cm long, were assembled into a bundle. The fibers

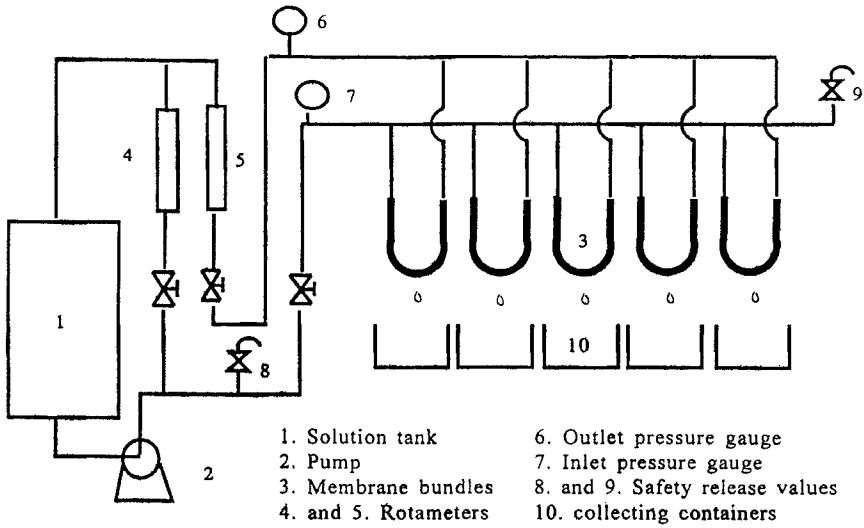

FIG. 3 Schematic diagram of hollow fiber membrane test system.

were glued at the bundle ends with epoxy adhesive. Each end was then potted into a 1/4 inch diameter polypropylene (3 cm long) tube section. The glue was then allowed to set at normal laboratory environment for at least 3 hours, keeping the unpotted parts of the fibers under water. The bundles were then stored in deionized water overnight. The potted bundle was then ready for attachment to the test rig.

Referring to Fig. 3, a circulating pump (2) was used to pump the feed solution in tank (1), under pressure, through a rotameter (5) into the bores of the fiber bundles whose inlet and outlet pressures were indicated by the gauges (7) and (6), respectively. The fluid that permeated through the fiber walls was collected in containers (10) and weighed. The PWP and PR are calculated on the basis of the bore side surface area of the fibers used. The PEG concentrations in the feed and permeate solutions were determined using a Shimadzu TOC-500 Total Organic Carbon Analyzer. The UF separations of PEG solutes were calculated from the following equation:

$$f\ (\%) = 100 \times [(\text{solute ppm in feed} - \text{solute ppm in permeate})/\text{solute ppm in feed}]$$

Because of the very low solute concentration involved, the PWP and PR data were essentially the same in all the experiments, and hence only the PR data are reported in this paper.

Several fibers were produced in this work under different spinning conditions, and they are designated in this report both by the composition of the fiber spinning solution (C1 or C2) followed by three numbers indicating WFR (mL/min), LAG (cm), and EP (psig), respectively.

RESULTS AND DISCUSSION

Effects of WFR and LAG in the Production of C1 and C2 Fibers

Phase Inversion Process

The formation of hollow fiber UF membranes by the solution spinning technique used in this work is a phase inversion process similar to the formation of the original flat sheet cellulose acetate RO membranes (15). In the latter case the initial solvent removal (desolvation) from the surface of the membrane during formation, and the consequent skin layer formation on the surface of the incipient membrane, are accomplished by the solvent evaporation step; in the fiber spinning process the same result is accomplished by the combination of WFR, LAG, and EP used. More particularly, the water flow velocity WFV through the bore of the fiber during formation and the water flow period WFP (i.e., the desolvation period = LAG/WFV) primarily govern the bore side skin layer morphol-

ogy and hence the UF performance characteristics of the resulting fiber. Further, WFR, LAG, and EP, and hence the corresponding WFV, WFP, and NFV, also contribute significantly to the ultimate dimensional characteristics (OD and ID) of the resulting fiber. These considerations form the basis for reviewing the experimental results obtained in this work not only in terms of WFR, LAG, and EP but also in terms of WFV, WFP, and NFV, particularly in view of the fact that extensive data are available in the literature (15), for comparison, on the effects of solvent evaporation rate (related to WFV), solvent evaporation period (related to WFP), and film-casting speed (related to NFV) on the performance characteristics of flat sheet RO membranes obtained by the phase inversion process.

Fiber Production Variables

In both the C1 and C2 spinning solutions (Table 1), the polymer concentration (P) was the same, but the PVP concentration (N) was higher and the NMP concentration (S) was correspondingly lower in C2 than in C1 solution. The S/P, N/S, and N/P ratios were 3.75, 0.0667, and 0.25, respectively, for C1 solution; the corresponding ratios for C2 solution were 3.5, 0.1428, and 0.5, respectively. Because of the higher PVP concentration in C2 solution, its viscosity was considerably higher than that of C1 solution. The EP used for the production of C1 fibers was 5 psig while that used for the production of C2 fibers was 15 psig. WFR values of 5 and 7.5 mL/min were used in the production of both C1 and C2 fibers. The experimental results obtained for C1 and C2 fibers are given in Figs. 4 to 12.

Fiber Dimensions

The OD and ID values of polymer hollow fibers obtainable by the solution spinning techniques are function of polymer solution structure (apparent viscosity), details of spinnerette design (values of OD_{Fix} and ID_{Fix}), extrusion pressure (NFV), WFR, and LAG. Explicit mathematical expressions for OD and ID as functions of the above variables have not been established. The object of the present study is only to examine the trends in the variations of OD and ID obtained experimentally in this work as functions of WFR, LAG, WFV, WFP, and NFV.

In the range of WFR and LAG values studied, with respect to C1 fibers the data on OD were in the 0.75 to 1.12 mm range, those on ID were in the 0.44 to 0.71 mm range, and those on wall thickness were in the 0.15 to 0.23 mm range; with respect to C2 fibers, the corresponding ranges were 1.10 to 1.42 mm for OD, 0.73 to 0.92 mm for ID, and 0.15 to 0.26 mm for wall thickness. Thus the effect of higher solution viscosity, together with higher extrusion pressure, was essentially to increase both OD and ID significantly.

Figure 4 shows that for both C1 and C2 fibers, an increase in WFR at a given LAG tends to increase OD and ID, and decrease wall thickness and OD/ID ratio; and increase in LAG, at a given WFR, tends to decrease OD, ID, and wall thickness whereas, depending on the magnitude of the above changes, the OD/ID ratio may pass through a slight maximum, or remain essential constant, or decrease. The decrease in wall thickness with an increase in LAG is steeper for C2 fibers compared to C1 fibers; this result indicates the existence of more than one effect, and the relative intensification of one effect more than the others.

As pointed out earlier, the variations of OD and ID as functions of WFR and LAG may also be reviewed from the points of view of WFV and WFP during the desolvation process. It is recognized that WFV will in general be nonuniform throughout the length of the incipient fiber because of the changing ID values with LAG. However, the use of the ID value of the

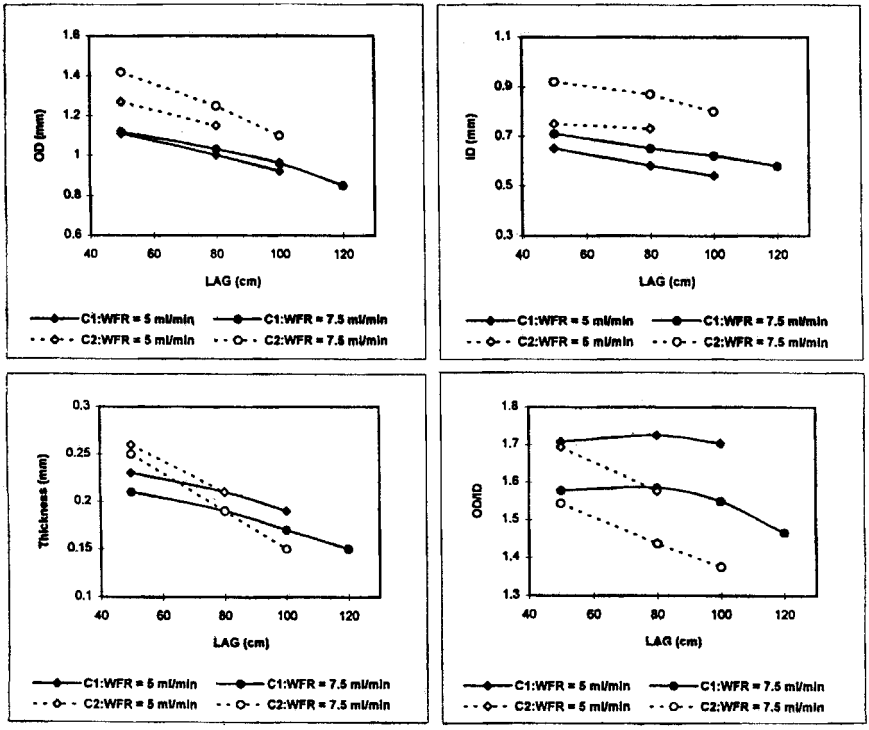

FIG. 4 Effects of LAG and WFR on C1 and C2 fiber dimensions.

fully coagulated fiber to calculate WFV and WFP can be expected to yield mutually relative values for each of these variables, which can then be used to examine the trends involved in the variations of OD and wall thickness in the process of fiber production. On the above basis, for the purpose of this discussion, WFV and WFP were defined as follows:

$$\text{WFV} = 4\text{WFR}/\pi(\text{ID})^2 \quad \text{and} \quad \text{WFP} = \text{LAG}/\text{WFV}$$

It may be noted that values of OD and wall thickness are not explicitly involved in the above definitions.

As a consequence of the above definitions, different combinations of WFR and ID (i.e., LAG) values can yield identical values for WFV or WFP.

In Fig. 5 the experimental data on OD and wall thickness given in Fig. 4 are replotted as functions of WFV and WFP. The results show that:

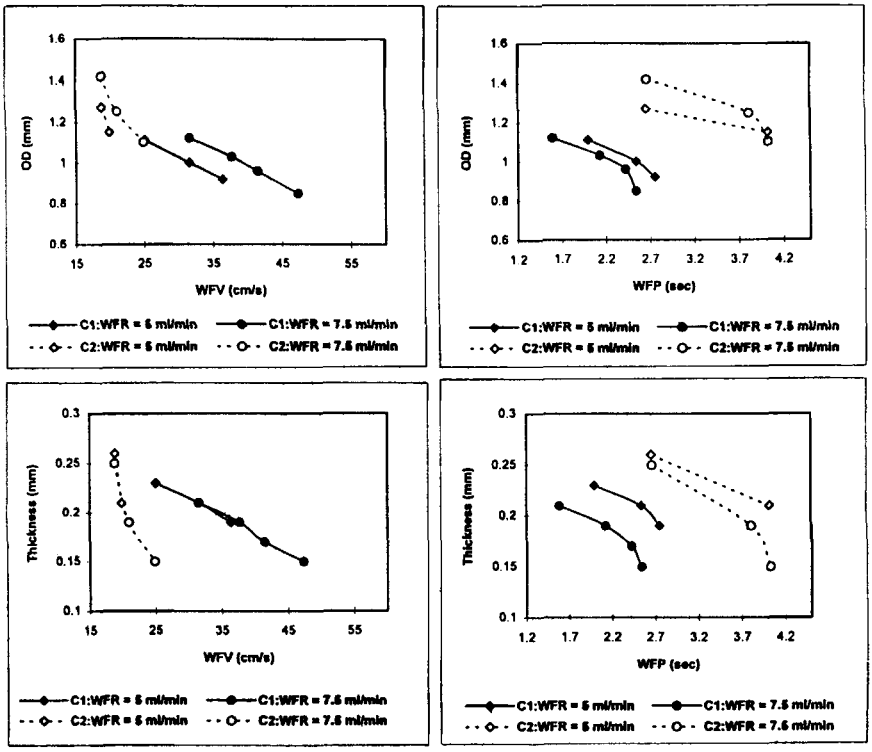

FIG. 5 Effects of WFR, WFV, and WFP on C1 and C2 fiber dimensions.

(a) correlations exist among WFV, WFP, and the resulting OD and wall thickness of the fibers produced, indicating that the above variables are indeed related; (b) an increase in WFV and also an increase in WFP tend to decrease the OD and wall thickness for both the WFR studied; but the rates of such decreases have different slopes, indicating the result of some compounding or competing effects; (c) at any given WFV, higher WFR tends to increase OD and decrease wall thickness; (d) at any given WFP, higher WFR tends to decrease OD for C1 fibers and increase OD for C2 fibers; however, higher WFR tends to decrease the wall thickness for both C1 and C2 fibers at any given WFP.

The above results are understandable on the following basis.

Using the FT-IR–IRS technique, Miyano et al. have shown (17) that in PES–PVP–DMSO film-casting solutions, part of the PVP remains bound to PES, such bound PVP is not water leachable, and the fraction of PVP so bound to PES increases with an increase in the PVP/(PVP + PES) weight ratio. This may also be the case with respect to PES–PVP–NMP solutions used for fiber spinning in this work, which would then mean that a fraction of PVP in the fiber spinning solution remains bound to PES in both C1 and C2 solutions, and the fractional amount of such bound PVP is more in the C2 solution than in the C1 solution. Since PVP is highly hydrophilic, the bound PVP also has the capacity to interact and absorb the internal coagulant water (WFR) and swell the fiber during formation.

Consequently, the WFR used in fiber spinning performs three major functions; they are 1) desolvation, i.e., the removal of NMP and unbound PVP in the spinning solution from the bore side of the fiber, giving rise to skin layer formation; 2) interaction with the bound PVP, resulting in absorption of water and swelling of fiber during its formation; and 3) viscoelastic deformation of the fiber due to high WFR (lateral fiber stretching). These three functions—namely desolvation, fiber swelling, and fiber stretching—may have compounding or competing effects on the ultimate fiber dimensions and also fiber performance.

Desolvation tends to decrease OD, ID, and wall thickness of the resulting fibers; fiber swelling tends to increase OD and wall thickness but decreases ID; fiber stretching tends to increase OD and ID but decreases wall thickness when WFR is sufficiently high.

The desolvation effect is enhanced by higher NMP and/or PVP content in the polymer solution and also by higher WFR during fiber production. The fiber swelling effect is enhanced by higher bound PVP content in the polymer solution and also by higher WFR. The fiber-stretching effect is enhanced by higher WFR. Thus higher WFR tends to enhance all three effects to different extents depending on fiber production conditions.

At any given WFR an increase in WFV tends to increase the desolvation rate, and consequently to decrease OD and wall thickness; but these changes tend to diminish with any further increase in WFV because of progressive increase in skin layer rigidity and the consequent decrease in the extent of water penetration into the interior of the fiber wall. This explains the declining slope of the OD vs WFV correlation shown in Fig. 5.

At any given WFV the increase in OD at higher WFR can be attributed partly to fiber swelling and partly to fiber stretching.

At any given WFR the decrease in wall thickness with an increase in WFV can be attributed to the increase in desolvation rate. The steeper decrease in wall thickness with increase in WFV with respect to the C2 fibers is also attributable to the increase in desolvation effect because of the higher unbound PVP concentration in the polymer solution.

At any given WFR an increase in WFP facilitates more desolvation to take place, and hence decreases OD as well as wall thickness. At a given WFP the OD values are higher for C2 fibers than those for C1 fibers because of the greater fiber swelling effect for C2 fibers as a consequence of the higher bound PVP concentration in C2 solution. The above fiber swelling effect tends to be more at higher WFR. On the other hand, the desolvation effect is more dominant for C1 fibers because of the higher NMP content and lesser bound PVP content in C1 solution; the above desolvation effect is more at higher WFR, and hence the resulting OD is smaller at higher WFR at higher WFR at any given WFP.

With respect to wall thickness, C2 fibers are thicker than C1 fibers because of the greater fiber swelling effect (for the reason given above), and the thickness decreases with an increase in WFP because of more desolvation which is further enhanced at higher WFR.

Thus all the different kinds of variations shown in Fig. 5 are well understood.

Nascent Fiber Velocity

Just like fiber dimensions, the NFV obtainable in fiber spinning is also a function of polymer solution structure (apparent viscosity), extrusion pressure (EP), details of spinnerette design (OD_{Fix} and ID_{Fix}), WFR, and LAG. Again, no explicit mathematical expression for NFV involving the above variables has yet been established. However, it is reasonable to expect correlations to exist among NFV and the various fiber production variables and fiber dimensional characteristics. The experimental results confirm that such is indeed the case.

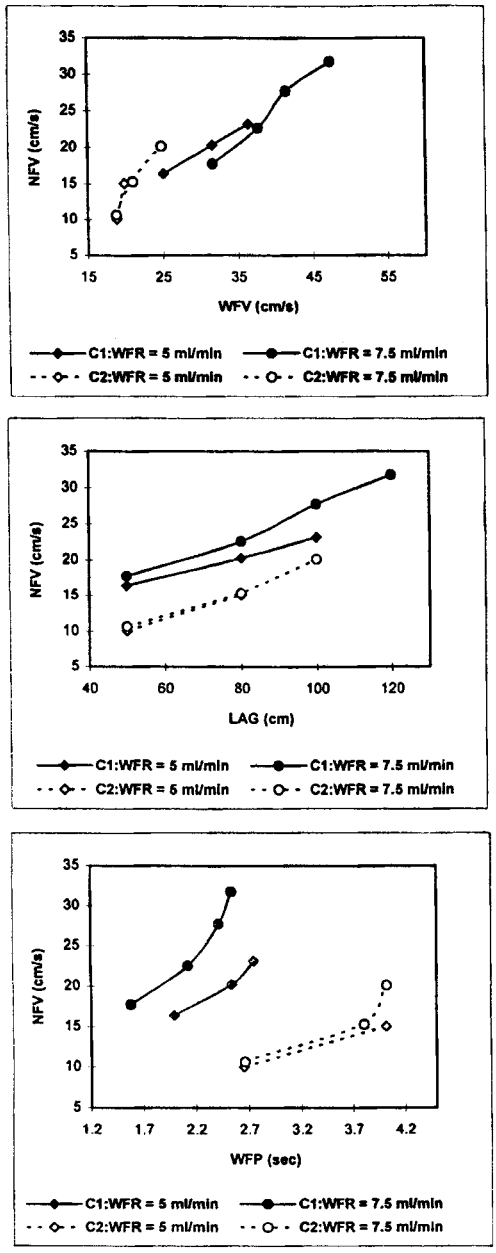

FIG. 6 Effects of LAG, WFV, WFP, and WFR on NFV for C1 and C2 fibers.

In the range of WFR and LAG studied, the data on NFV were in the 16.4 to 31.8 cm/s range for C1 fibers and the 10.1 to 20.1 cm/s range for C2 fibers. Thus the NFV values were significantly lower for C2 fibers (in spite of the higher EP used), indicating the dominant effect of solution structure, including the high viscosity of the polymer solution.

Figure 6 shows that for both C1 and C2 fibers, NFV increases with an increase in LAG, WFV, or WFP; further, at any given LAG, WFV, or WFP, an increase in WFR tended to increase NFV, but the latter tendency was more for C1 fibers than for C2 fibers. These results indicate that while all three events taking place during fiber formation—namely, desolvation, fiber swelling, and fiber stretching—affect NFV, desolvation has the dominant effect on NFV. An increase in desolvation rate (WFV) and also an increase in the extent of desolvation (WFP) tend to increase NFV.

The above conclusion is supported by the correlations presented in Fig. 7 which show the effect of NFV on OD, ID, wall thickness, and OD/ID

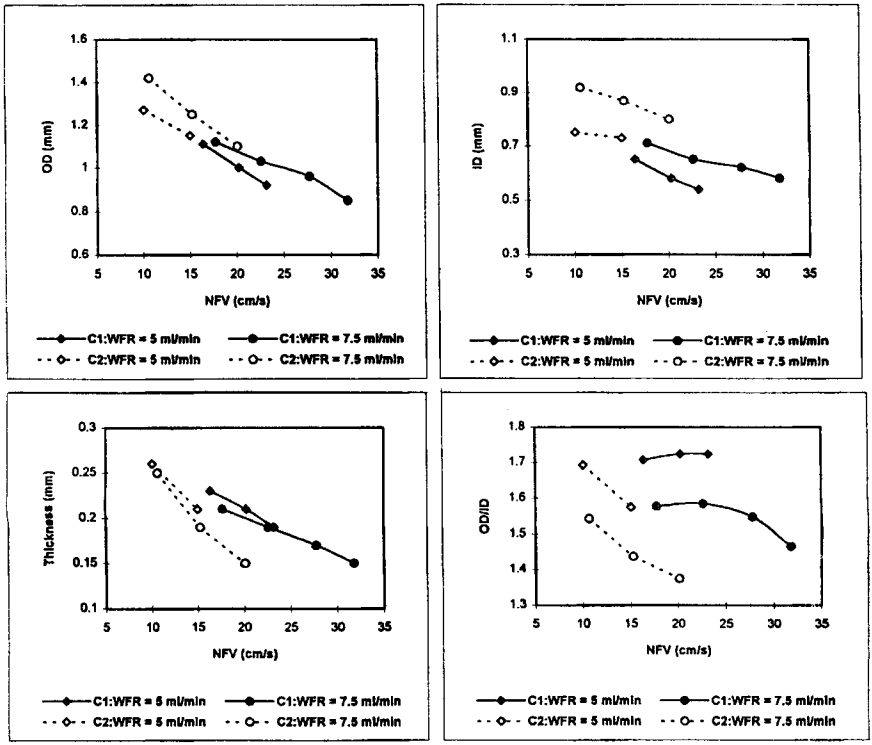

FIG. 7 Effects of NFV and WFR on C1 and C2 fiber dimensions.

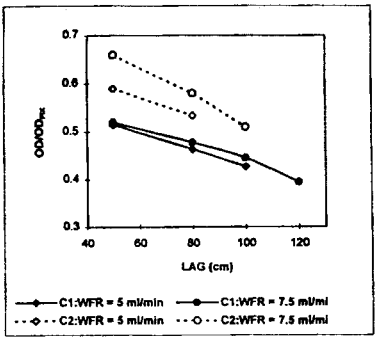

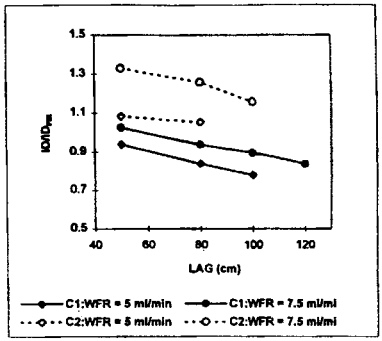

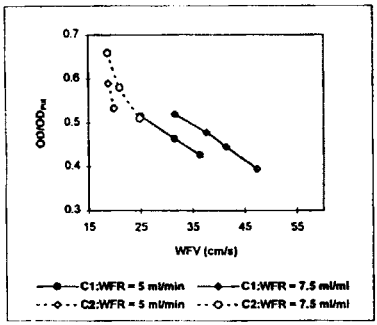

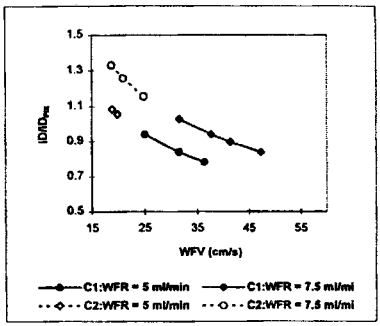

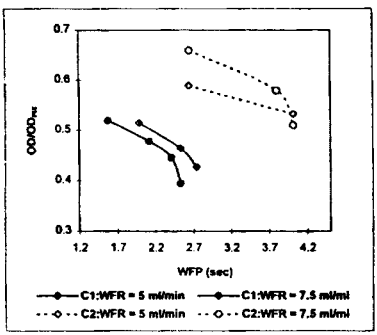

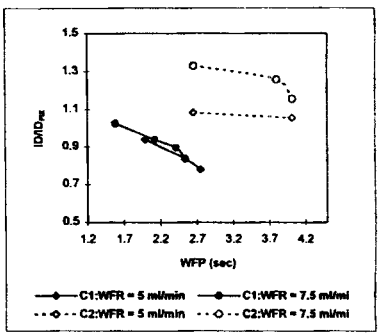

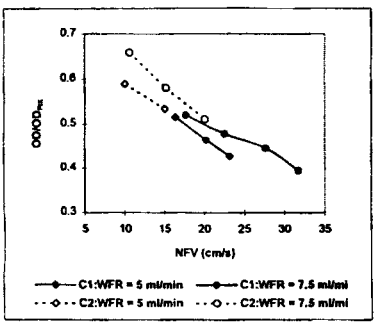

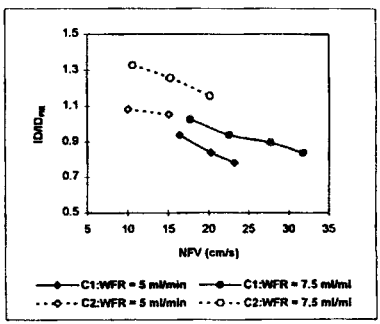

ratio. These correlations are similar to those shown in Fig. 4, which is only to be expected in view of the LAG vs NFV correlation given in Fig. 6. Figure 7 shows that at any given WFR, an increase in NFV decreases OD, ID, and wall thickness, indicating the dominant effect of desolvation. The decrease in ID with an increase in NFV is less steep because of the higher rigidity of the skin layer on the bore side of the fiber. The decrease in thickness with an increase in NFV is steeper for C2 fibers because of the enhanced desolvation effect due to the higher unbound PVP content in C2 solution. The variations in OD/ID simply follow the corresponding variations in OD and ID. At any given NFV the effect of higher WFR on OD, ID, and wall thickness is to enhance the desolvation, and, to a lesser extent, the fiber swelling and fiber stretching effects, as discussed earlier.

Spinnerette Design and Fiber Dimensions

Figure 8 illustrates the effect of one aspect of spinnerette design (OD_{Fix} and ID_{Fix} shown in Fig. 2) on the resulting fibers dimensions. Since the values of OD_{Fix} and ID_{Fix} are constants fixed by the spinnerette design, the correlations of OD/OD_{Fix} and ID/ID_{Fix} as functions of LAG, WFR, WFV, WFP, and NFV are similar to the corresponding correlations given in Figs. 4, 5, and 7 which have already been discussed. The objective of Fig. 8 is to show that in all the cases studied the values of OD/OD_{Fix} are always less than unity, while those of ID/ID_{Fix} can be equal to, higher than, or less than unity, depending on the fiber production conditions.

Fiber Performance in UF Experiments

Figures 9(a) and 9(b) show the effects of WFR and LAG on PEG separations and PR for C1 and C2 fibers, respectively. Because of the very low solute concentration (~100 ppm) used in PEG aqueous feed solutions, the PR data obtained were essentially the same for all the feed solutions tested; the PR data reported here are the average values from the feed solutions involving PEG solutes with different molecular weights tested under the average operating pressure of 20 psig at a laboratory temperature of ~24°C.

The solute separation and PR data are mutually independent. They are well understood in terms of the morphology (overall porous structure) and productivity (PR for a given level of solute separation) characteristics of the fibers tested. With reference to a given solute, a higher level of UF separation indicates a smaller average size of pores on the skin layer of

FIG. 8 Effects ot LAG, WFR, WFV, WFP, and NFV on OD/OD_{Fix} and ID/ID_{Fix} for C1 and C2 fibers.

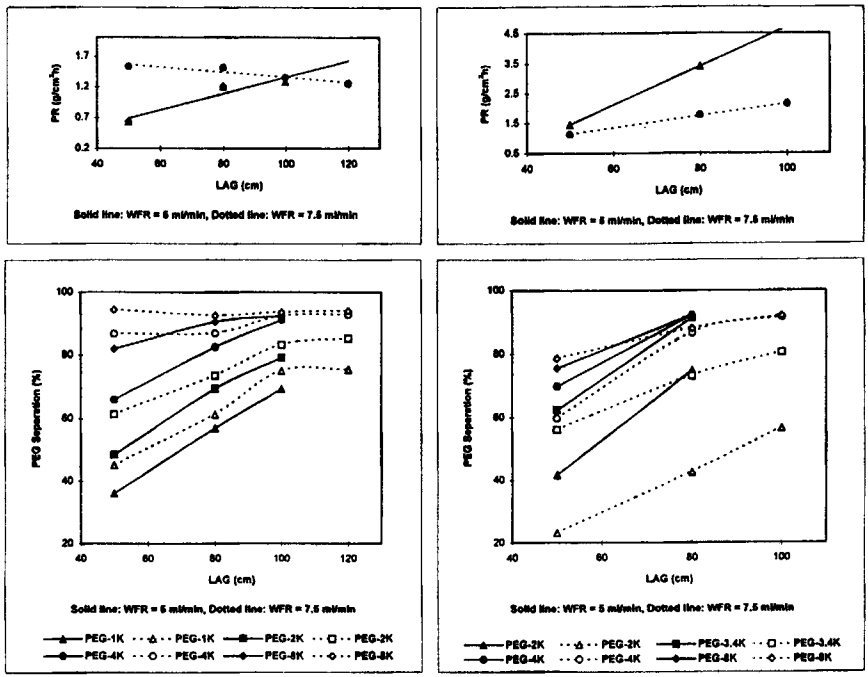

(a) C1 fibers (b) C2 fibers

FIG. 9 Effects of WFR and LAG on UF performance of C1 and C2 fibers.

the bore side surface of the fiber. A higher PR can be the result of one or more of the following factors: bigger average pore size on the skin layer, larger number of pores on the skin layer, thinner skin layer, and/or greater asymmetricity of the overall pore structure of the fiber wall.

The conditions under which the resulting fiber yields both high solute separations and high PR are of particular interest from the point of view of fiber morphology. Such a simultaneous increase in both solute separations and PR is indicative of a simultaneous decrease in the average size of skin layer pores and an increase in the effective number of such pores on the skin layer of the bore side surface of the fiber. The term "increase in effective number of such pores" used above includes the possible increase in the number of skin layer pores, thinner skin layer, and greater asymmetricity of the overall porous structure of the fiber wall.

Factors Governing the Development of Skin Layer Pore Structure during Fiber Formation

The solution structure desolvation rate approach, discussed extensively in the literature (15) with reference to the development of skin layer pore structure during the formation of flat cellulose acetate RO/UF membranes, is also applicable to the development of skin layer pore structure during the formation of hollow fiber membranes produced in this work. Further, the concepts of polymer network pores and aggregate pores, nonsolvent droplet formation, and droplet coalescence in the interdispersed phase during skin layer formation, the effects of coagulation kinetics of polymer dispersions on membrane morphology, and the important part played by the nonsolvent additive (for example, PVP in this work) in pore formation and development, discussed in the literature (15), are also relevant to an understanding of the factors governing the ultimate skin layer pore structure of the hollow fiber membranes produced under different desolvation conditions.

In addition to the effect of polymer solution structure, the desolvation conditions during fiber production in this work also include the simultaneous fiber swelling and fiber stretching events, all of which together govern the final skin layer pore structure of the resulting fiber.

From the point of view of the polymer solution structure, since the *S*/*P* ratio is lower, the *N*/*S* and *N*/*P* ratios are higher for C2 solution than those for C1 solution, one would expect—in the absence of other effects—that the supermolecular polymer aggregates in C2 solution will be bigger in size and smaller in number; consequently the aggregate pores of C2 fibers may be expected to be bigger in size and smaller in number compared to those of C1 fibers. On the other hand, the PES–PVP interaction in PES–PVP–NMP solution may be analogous to the cellulose acetate-formamide interaction in cellulose acetate-formamide-acetone solution (15, 18), in which case the PES–PVP interaction will favor the formation of a more extensive polymer network structure in the interdispersed skin layer phase during fiber formation, giving rise to more numerous smaller skin layer pores; such PES–PVP interaction appears to be the case for C2 fibers.

Of the three events taking place during fiber formation, namely, desolvation, fiber swelling, and fiber stretching, the rate and extent of desolvation may be expected to have the major effect on skin layer morphology, i.e., skin layer thickness and pore size, pore size distribution, and pore density on the skin layer. Under certain conditions the effects of the other two events may also be significant.

TABLE 2
Effects of Desolvation, Fiber Swelling, and Fiber Stretching on Skin Layer Morphology

Skin layer morphology characteristics	Desolvation: Increase in WFR (up to a limit)	Desolvation: Too much increase in WFR	Fiber swelling	Fiber stretching
Skin layer thickness	Decrease	Increase	Increase	Decrease
Average pore size	Decrease	Increase	Increase/decrease /no change	Increase
Pore density (number of pores/unit area)	Increase	Decrease	Decrease	Decrease
Pore size distribution	Narrower	Wider	Wider	Wider

On the basis of the extensive experimental results reported and discussed with respect to the production of flat-sheet RO/UF membranes (15), the desolvation, fiber swelling, and fiber stretching effects during hollow fiber membrane production may be expected to have the following qualitative effects on the skin layer morphology of the resulting fibers as shown in Table 2.

The tendencies indicated in Table 2 need extensive experimental verification under different production conditions.

For a given fiber spinning solution and extrusion pressure, since different conditions of WFR and LAG can give rise to the same WFV or WFP, such combinations can also give rise to the same average pore size on the skin layer of the resulting fiber (i.e., same solute separation in UF); but the above combinations need not have the same pore density (resulting in the same PR in UF) on the skin layer since the factors governing average pore size and pore density are not identical in fiber production. Table 2 indicates the possibility of identifying experimental conditions (polymer solution structure, EP, WFR, and LAG) under which both solute separations and PR can be increased simultaneously, and also the means for shifting the MWCO values (i.e., the morphology characteristics of the skin layer) for the fibers produced.

Data on UF Performance of C1 and C2 Fibers

Data on C1 Fibers

Figure 9(a) shows that, for the case of WFR = 5 mL/min, an increase in LAG tended to increase PEG separations (i.e., a decrease of the average

pore size) and also to increase PR, indicating simultaneous generation of a larger number of smaller size pores on the skin layer and a decrease in the skin layer thickness. At WFR = 7.5 mL/min, an increase in LAG tended to increase PEG separations (i.e., a decrease in the average pore size) but to decrease PR which can be attributed, at least in part, to the decrease in average pore size. At LAG = 50 cm, an increase in WFR from 5 to 7.5 mL/min increased PEG separations (i.e., a decrease in the average pore size) and also increased PR more than twofold, indicating that increased WFR, together with lower LAG, tended to generate both smaller size pores on the skin layer and a thinner skin layer. At LAG of 100 cm, an increase in WFR still decreased the average pore size but did not change PR, which again indicates a simultaneous decrease in average pore size and skin layer thickness. All the above observations are consistent with the conclusion that desolvation was the major factor governing skin layer morphology for C1 fibers, and an increase in WFR as well as an increase LAG tended to generate a larger number of smaller size pores on the skin layer, and also to decrease the skin layer thickness because of the increase in the extent and rate of desolvation.

The above results also illustrate that different combinations of WFR and LAG can give the same solute separation (i.e., same average pore size) but different PR for the resulting fibers. For example, considering PEG-2K solute, interpolation of data in Fig. 9(a) shows that for the fibers obtained from WFR-LAG combination of 7.5–50 and 5–66 could have the same solute separation of 61%, but the PR value for the former fiber could be more than 50% higher than that for the latter.

The combined effect of WFR and LAG indicated above is also of further interest. Arbitrarily defining the "molecular weight cut off (MWCO)" characteristic of the hollow fiber membranes as the molecular weight of PEG for which the solute separation under the specified UF operating conditions is 90% or above, the following data illustrate the combined effect of WFR and LAG on the MWCO characteristic of the hollow fiber membranes produced as shown in Table 3.

TABLE 3
Combined Effects of WFR and LAG on MWCO of Some C1 Fibers

Fiber	MWCO of PEG solute	Solute separation (%)	PR ($g/cm^2 \cdot h$)
C1-5-80-5	PEG-8K	90.5	1.21
C1-5-100-5	PEG-4K	91.1	1.28
C1-7.5-100-5	PEG-3.4K	91.1	1.35

Table 3 shows that the MWCO value tends to decrease (i.e., the average pore size on the skin layer tends to decrease) by an increase in WFR and/or LAG. A lower MWCO, together with a higher PR, indicates not only a smaller average size of skin layer pores but also an increase in the effective number of such pores on the skin layer of the resulting fiber (for example, C1-7.5-100-5).

Among C1 fibers studied, the performance characteristics of C1-7.5-50-5 and C1-7.5-120-5 fibers are typically illustrative as shown in Table 4. Data given in Table 4 indicate that an increase in LAG at constant WFR decreases the average pore size on the skin layer and also decreases PR for the resulting fiber.

Further, Fig. 9(a) shows that as LAG increased, the differences in PEG separations and PR tended to decrease for the resulting fibers at both WFR of 5 and 7.5 mL/min. For example, at WFR = 5 mL/min, an increase in LAG from 50 to 100 cm increased the separation of PEG-2K from 48.5 to 79.2%, that of PEG-4K from 66.0 to 91.1%, and that of PEG-8K from 82.0 to 92.2%; under the above experimental conditions, the PR values increased from 0.64 to 1.28 g/cm^2·h, representing an increase of 100%, while the fiber wall thickness decreased by only 17% (from 0.23 to 0.19 mm). On the other hand, at WFR = 7.5 mL/min, an increase in LAG from 50 to 100 cm increased the separation of PEG-2K from 61.3 to 83.3% and that of PEG-4K from 86.8 to 92.4%, while there was practically no change in the separation of PEG-8K (~94%); under the above experimental conditions, the PR values decreased from 1.53 to 1.35 g/cm^2·h, representing a decrease of 12%, while the corresponding fiber wall thickness decreased by 19% (from 0.21 to 0.17 mm).

The above data indicate that an increase in LAG from 50 to 100 cm decreased the size of the skin layer pores at both the WFR values studied, but the relative decrease was more for the smaller pores than for the bigger pores. They also indicate that WFR and LAG have independent effects on fiber morphology, and hence fiber performance. A change in the overall

TABLE 4
Effect of Increase in LAG at Constant WFR on the Performance of C1 Fibers

Fiber	PEG separations (%)				PR (g/cm^2·h)
	2K	3.4K	4K	8K	
C1-7.5-50-5	61.3	82.4	86.8	94.4	1.53
C1-7.5-120-5	85.3	91.5	92.8	94.0	1.25

fiber wall thickness is not a major factor in the resulting PR which is determined primarily by the morphology of the skin layer pore structure on the bore side surface of the fiber.

Data on C2 Fibers

Figure 9(b) shows that both PEG separation and PR increased with an increase in LAG and a decrease in WFR for C2 fibers. These results, which are different from those obtained with C1 fibers, indicate that, in addition to desolvation, there could be additional factors governing the morphology of the skin layer of C2 fibers during production. These additional factors should naturally include the higher EP used in the production of C2 fibers and the higher PVP content (and the consequent higher bound PVP content) in C2 fiber spinning solution.

It has already been pointed out that the fiber swelling effect was relatively greater in the production of C2 than that of C1 fibers because of the higher bound PVP content in C2 spinning solution, and the above fiber swelling effect could be enhanced at higher WFR. While the desolvation effect (which is still the major effect governing the skin layer morphology) tends to decrease pore size and increase pore density, the fiber swelling effect tends to increase pore size and decrease pore density in the skin layer of the fiber during formation. Therefore, the data presented in Fig. 9(b) can be understood on the basis that an increase in LAG intensifies the desolvation effect, and an increase in WFR intensifies both desolvation and fiber swelling effects.

The above results also illustrate that different combinations of WFR and LAG can give the same solute separation (i.e., the same average pore size) but different PR for the resulting fibers. For example, again considering PEG-2K solute, interpolation of data in Fig. 9(b) shows that for the fibers obtained from the WFR-LAG combinations of 5–58 and 7.5–92 could have the same solute separation (50%), but the PR value for the latter could be about 20% higher than that for the former. Thus for a given level of solute separation (i.e., the same average pore size on the skin layer), PR increased for the combination of higher WFR and lower LAG for C1 fibers, and for the combination of higher WFR and higher LAG for C2 fibers. There is, however, no contradiction here because, in both cases, higher PR were obtained for the combination of higher WFR and higher WFV through the fiber bore during fiber formation.

The combined effect of WFR and LAG is again of particular interest from the point of view of the MWCO of C2 fibers produced. C2-5-80-15 fiber had a MWCO for PEG-3.4K with a PR value of 3.41 g/cm^2·h, which is more than 2.5 times that obtained for the comparable fiber C1-7.5-100-

TABLE 5
Production and Performance Characteristics of Two Fibers with MWCO for PEG-3.4K

Characteristics	Fibers	
	C1-7.5-100-5	C2-5-80-15
WFV, cm/s	41.40	19.91
WFP, s	2.42	4.02
NFV, cm/s	27.73	15.10
OD, mm	0.96	1.15
ID, mm	0.62	0.73
Wall thickness, mm	0.17	0.21
OD/ID	1.55	1.58
Solute separation, %:		
PEG-3.4K	91.1	91.3
PEG-4K	92.4	92.1
PEG-8K	93.7	92.2
PR, $g/cm^2 \cdot h$	1.35	3.41

5 pointed out earlier. In view of the potential industrial utility of the above two fibers, their production details, dimensions, and performance characteristics are listed in Table 5.

Effects of WFV, WFP, and NFV

The data on C1 and C2 fibers discussed above may also be considered from the points of view of the effects of WFV, WFP, and NFV on the skin layer morphology of the fibers produced. Figures 10, 11, and 12 show the correlation of WFV, WFP, and NFV, respectively, with PEG separations and PR for C1 and C2 fibers included in Fig. 9. For both the above groups of fibers, under the experimental conditions used in their production, for each WFR, an increase in LAG also increased the magnitude of WFV, WFP, and NFV. Consequently, the correlations shown in Figs. 10, 11, and 12 exhibit some similarities with those shown in Fig. 9. However, some additional observations are possible from the correlations given in Figs. 10, 11, and 12.

Figure 10 shows that for both C1 and C2 fibers, at constant WFR, an increase in WFV tends to increase solute separation or to decrease average pore size on the skin layer; on the other hand, at any given WFV, an increase in WFR tends to decrease solute separation or to increase the

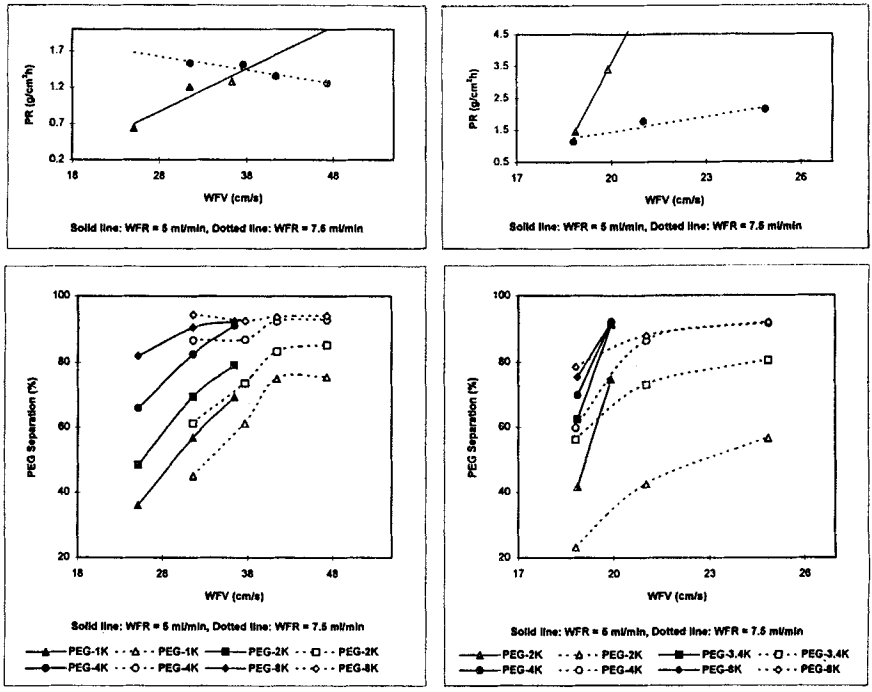

(a) C1 fibers (b) C2 fibers

FIG. 10 Effects of WFR and WFV on UF performance of C1 and C2 fibers.

average pore size on the skin layer. Consequently, a higher WFV together with a lower WFR tends to result in smaller size pores on the skin layer of the fiber. Further, the same average pore size (i.e., same solute separation) can be obtained by an appropriate combination of a lower WFV and a lower WFR, as well as a higher WFV and a higher WFR, but the latter combination tends to yield a higher PR, as already illustrated. The above results also indicate that WFV primarily governs the desolvation effect on skin layer morphology.

Figure 11 shows that for both C1 and C2 fibers at constant WFR, an increase in WFP tends to increase solute separations, i.e., decrease the average pore size on the skin layer; this is understandable because at constant WFR an increase in WFP also results in higher WFV. On the

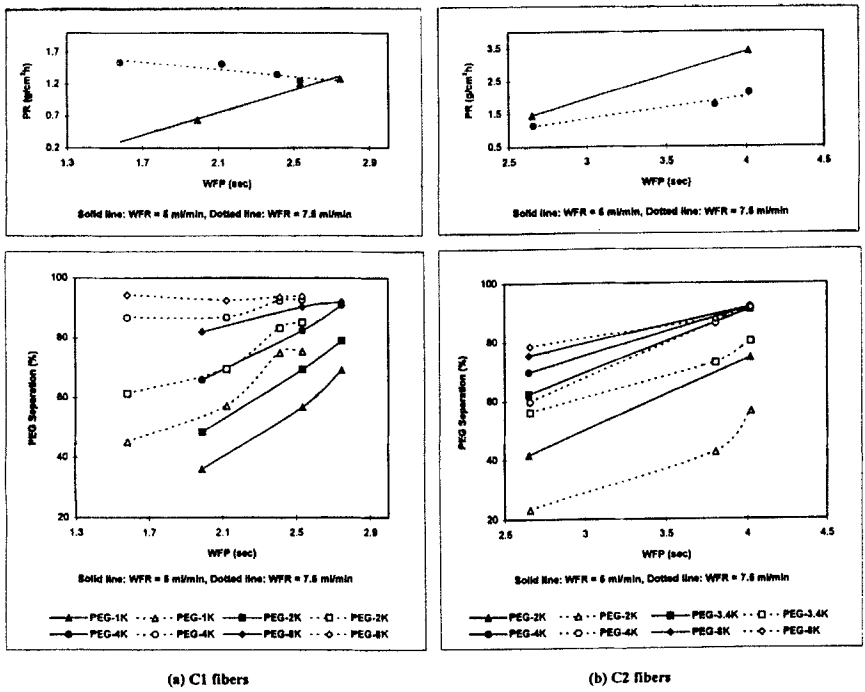

FIG. 11 Effects of WFR and WFP on UF performance of C1 and C2 fibers.

other hand, at constant WFP an increase in WFR tends to increase solute separation (i.e., decrease pore size) for C1 fibers and to decrease solute separation (i.e., increase pore size) for C2 fibers. This indicates that in the case of C1 fibers an increase in WFR intensifies the desolvation effect, whereas in the case of C2 fibers an increase in WFR intensifies both the desolvation and fiber swelling effects. Furthermore, the results also show that the same average pore size (i.e., same level of solute separation) is obtainable by an appropriate combination of higher WFR and lower WFP, or lower WFR and higher WFP for C1 fibers, whereas similar results are possible by appropriate combinations of lower WFR and lower WFP or higher WFR and higher WFP for C2 fibers. The above results also indicate that WFP affects both desolvation and fiber swelling effects.

Figure 12 shows that for both C1 and C2 fibers, at constant WFR, an increase in NFV tends to increase solute separation, i.e., decrease average

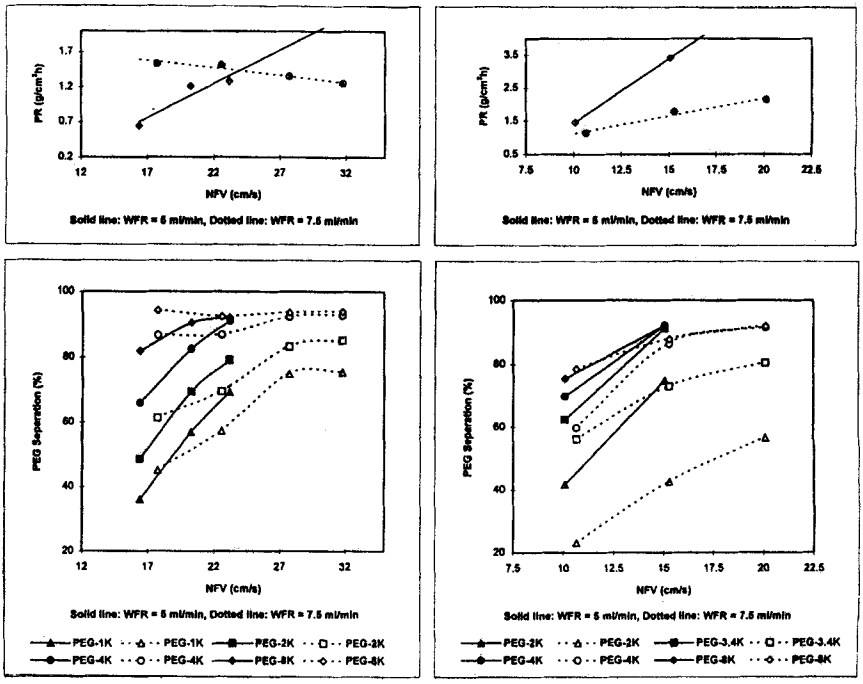

(a) C1 fibers (b) C2 fibers

FIG. 12 Effects of WFR and NFV on UF performance of C1 and C2 fibers.

pore size on the skin layer; this is again understandable since the data show that such an increase in NFV is also accompanied by an increase in WFV. On the other hand, at constant NFV, an increase in WFR tends to decrease solute separation i.e., increase the size of skin layer pores for both C1 and C2 fibers, which is attributable to the fiber stretching effect.

SEM Pictures

The wall cross sections of several C1 and C2 fibers were examined under a scanning electron microscope (SEM). Two typical SEM pictures are shown in Fig. 13. In all cases it was found that the fiber walls were asymmetrically porous, and the skin layer was on the bore side surface of the fiber.

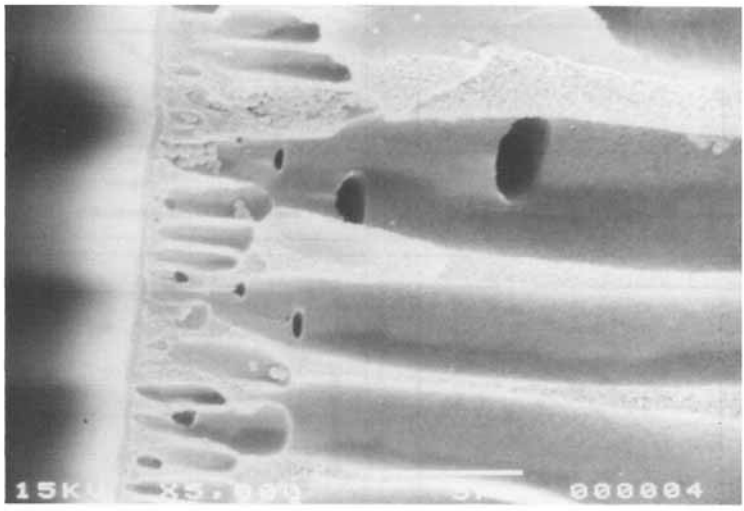

(a)

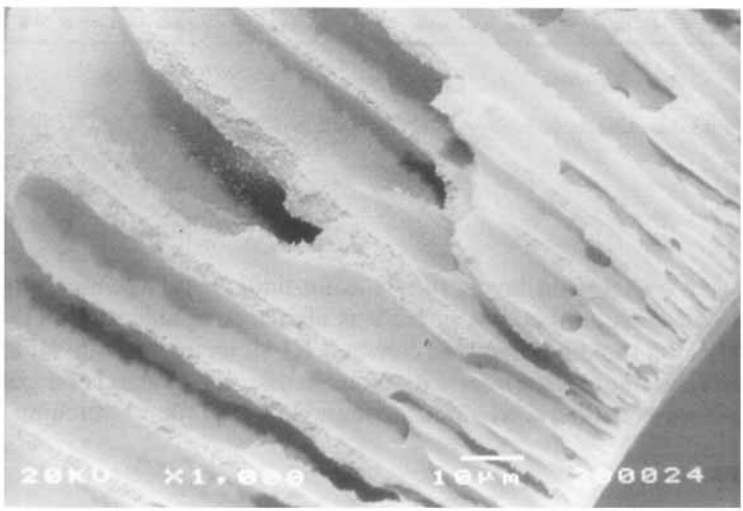

(b)

FIG. 13 Typical SEM pictures for the cross section of the bore side skin layer (a) C1-50-7.5-5 at magnification of 5000, and fiber asymmetrical wall (b) C2-80-5-15 at magnification of 1000.

CONCLUSIONS

The experimental data presented and discussed above lead to the following conclusions.

The effects of changes in WFR, LAG, WFV, WFP, and NFV on physical dimensions and UF performance of the resulting fibers are understandable on the basis of the physicochemical events of desolvation, fiber swelling, and fiber stretching taking place during fiber formation.

With regard to fiber dimensions, desolvation tends to decrease OD, ID, and wall thickness of the resulting fibers; fiber swelling tends to increase OD and wall thickness but to decrease ID; and fiber stretching tends to increase OD and ID and to decrease wall thickness. Higher WFR enhances all three effects to different extents depending on fiber production conditions. In addition, the desolvation effect is enhanced by higher NMP and/or unbound PVP content in the fiber spinning solution, and the fiber swelling effect is enhanced by higher bound PVP content in the fiber spinning solution.

UF performance of the resulting fibers is primarily a function of its skin layer morphology, which is again governed by the desolvation, fiber swelling, and fiber stretching events taking place during fiber production. An increase in WFR (up to a limit) tends to decrease the skin layer thickness and the size of the skin layer pores, but to increase pore density and narrow the pore size distribution on the skin layer. Fiber stretching also tends to decrease the skin layer thickness. Fiber swelling, fiber stretching, and too high a WFR tend to have opposite effects on skin layer morphology.

More experimental results on fiber production are still needed to identify the effects of spinning solution structure, spinnerette design, and the other variables of fiber production on the physical dimensions and UF performance of the resulting fibers in more precise terms.

REFERENCES

1. I. Cabasso, E. Klein, and J. K. Smith, *J. Appl. Polym. Sci.*, *20*, 2377 (1976).
2. I. Cabasso, E. Klein, and J. K. Smith, *Ibid.*, *21*, 165 (1977).
3. I. Cabasso, K. Q. Robert, E. Klein, and J. K. Smith, *Ibid.*, *21*, 1883 (1977).
4. I. Cabasso and A. P. Tamvakis, *Ibid.*, *23*, 1509 (1979).
5. I. Cabasso, "Hollow Fiber Membranes," in *Kirk–Othmer Encyclopedia of Chemical Technology* (M. Grayson and D. Eckroth, Eds.), Wiley, New York, 1980, p. 492.
6. I. Cabasso, "Hollow Fiber Membrane Research," in *Materials Science of Synthetic Membranes* (ACS Symp. Ser. 269, D. R. Lloyd, Ed.), American Chemical Society, Washington, D.C., 1985, p. 305.
7. R. Mckinney, Jr., *Desalination*, *62*, 37 (1987).

8. J. M. Espenan and P. Aptel, "Outer Skinned Hollow Fibers—Spinning and Properties," in *Membranes and Membrane Processes* (E. Drioli and M. Nakagaki, Eds.), Plenum, New York, 1986, p. 151.
9. T. Liu, S. Xu, D. Zhang, S. Sourirajan, and T. Matsuura, *Desalination*, *85*, 1 (1991).
10. T. Liu, D. Zhang, S. Xu, and S. Sourirajan, *Sep. Sci. Technol.*, *27*(2), 161 (1992).
11. H. Wood, J. Wang, and S. Sourirajan, *Ibid.*, *28*(15 & 16), 2297 (1993).
12. L. Brinkert, N. Abidine, and P. Aptel, *J. Membr. Sci.*, *77*, 123 (1993).
13. I. M. Wienk, H. A. Teunis, Th. v. d. Boomgaard, and C. A. Smolders, *Ibid.*, *78*, 93 (1993).
14. G. H. Koops, J. A. M. Nolten, M. H. V. Mulder, and C. A. Smolders, *J. Appl. Polym. Sci.*, *54*, 385 (1994).
15. S. Sourirajan and T. Matsuura, *Reverse Osmosis/Ultrafiltration Process Principles*, National Research Council of Canada, Ottawa, 1985, Chap. 6.
16. R. J. Petersen, *J. Membr. Sci.*, *83*, 81 (1993).
17. T. Miyano, T. Matsuura, D. J. Carlsson, and S. Sourirajan, *J. Appl. Polym. Sci.*, *41*, 407 (1990).
18. B. Kunst, D. Skevin, Gi. Dezelic, and J. J. Peters, *Ibid.*, *20*, 1339 (1976).

Received by editor May 15, 1995